New Journal of Physics
The open–access journal for physics

Effect of ionic size on the orbital ordering transition in $RMnO_{3+\delta}$

G Maris, V Volotchaev and T T M Palstra[1]
Solid State Chemistry Laboratory, Materials Science Centre, University of Groningen, Nijenborg 4, 9747 AG Groningen, The Netherlands
E-mail: palstra@chem.rug.nl

New Journal of Physics **6** (2004) 153
Received 25 June 2004
Published 5 November 2004
Online at http://www.njp.org/
doi:10.1088/1367-2630/6/1/153

Abstract. We present high-temperature powder x-ray diffraction data of the orbital-order-induced structural distortion of $RMnO_3$, with R a rare earth element. The associated phase transition takes place in a temperature interval of ≈200 K in which the orbitally ordered phase and the orbitally disordered phase coexist. We analyse the evolution of the $RMnO_3$ perovskite structure with the size of the rare-earth ion and with temperature. We show that the rotation of the MnO_6 octahedra stabilizes the cooperative Jahn–Teller distortion to higher temperature.

Contents

[1] Author to whom all correspondence should be addressed.

PII: S1367-2630(04)82588-6

1. Introduction

The rare-earth perovskites RTO_3, with R a rare-earth element and T a transition metal, have been intensively studied because of their wide variety in physical phenomena such as superconductivity, ferroelectricity and colossal magnetoresistance. In all these phenomena, the electronic properties are intimately related to the lattice. Many of the interesting phenomena involve a complex interplay between the spin, charge and orbital degrees of freedom, accompanied with subtle displacements in the crystal lattice. While it is commonly accepted that spin and charge determine the electronic properties in perovskites, it has become of recent interest to study the consequences of orbital degeneracy on physical properties.

In $RMnO_3$ perovskites, the degeneracy of the e_g orbital is removed by a cooperative Jahn-Teller (JT) distortion below a transition temperature T_{JT}. This distortion results in a long-range ordering of the occupied $3d_{3x^2-r^2}$ and $3d_{3y^2-r^2}$ orbitals. The most extensively studied compound throughout the $RMnO_3$ series, i.e. $LaMnO_3$, exhibits a structural phase transition at $T_{JT} \approx 800$ K [1, 2]. The orbital ordering induces changes in the crystal structure and has pronounced effects on the electronic properties. This transition is associated with drastic changes in the resistivity, thermo-electric power, and thermal conductivity [3]. This behaviour is associated with two consecutive transitions with decreasing temperature from an orbitally disordered, via a short-range ordered regime, $T^* < T < T_{JT}$, to a long-range orbitally ordered state [3]. Furthermore, these authors suggest that the phase transition changes from first order for $LaMnO_3$ to second order for smaller rare earth ions, i.e. $NdMnO_3$ and $PrMnO_3$ [3]. In contrast with the interpretation of these transport experiments, structural studies indicate that all the phase transitions are first order, with a varying temperature range of hysteresis [2, 4, 5]. Thus the nature of the phase transition and the effect of ionic size of the rare earth ion remain subjects to debate.

Although the room temperature (RT) crystal structure was studied in great detail [6, 7] for all the members of all the $RMnO_3$ compounds, the high-temperature structural behaviour has been much less analysed. It is clear from local probe techniques that local Jahn–Teller distortions persist above the ordering transition. In principle, the orbital order–disorder transition can be either first order, with no restriction on the symmetry relation between the two states, or second order, in which case the symmetry relation should be a group–subgroup relation. For the t_{2g}-based systems, a number of cases have been studied. Here, the orbital ordering takes place below room temperature. For various RVO_3 perovskites, the orbital order–disorder transition is second order, and at a distinctly different transition temperature than the magnetic ordering. The symmetry of the orbitally ordered state is still subject to intense study. For the $RTiO_3$ systems, the situation regarding the symmetry is less clear. For some systems, orbital ordering has been reported, but further studies seem necessary. For the e_g-based manganites both first- and second-order transitions have been reported. The situation is experimentally more easy, because the JT distortions are typically five times larger than for t_{2g}-based systems. It is widely accepted that for the manganites the orbital and magnetic ordering take place at different transition temperatures.

For a better understanding of the nature of the orbital ordering and the relationship with the electronic properties in $RMnO_3$, detailed high-temperature structural studies are of significant importance. Here, we present the results of the high-temperature structural study in $NdMnO_3$ using powder x-ray diffraction (PXD) experiments. Combining our work with earlier studies, we find that a smaller rare-earth ionic radius stabilizes the cooperative JT distortion to higher temperature in $RMnO_3$ perovskites.

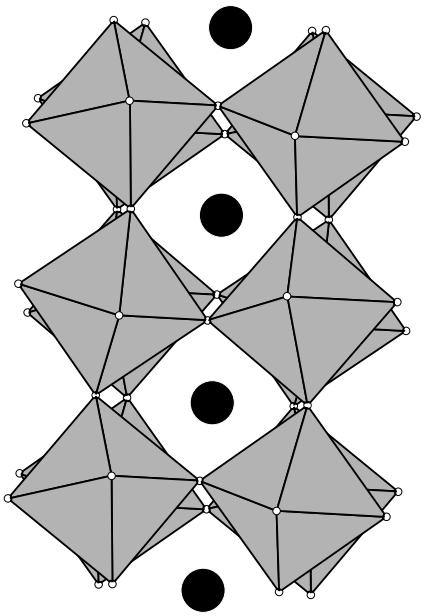

Figure 1. A general perovskite structure consisting of corner sharing octahedra. The octahedra consist of oxygen ions at the corners and Mn ions at the centre. The R ions occupy the voids between the octahedra.

2. Experimental procedures

Polycrystalline samples of $NdMnO_3$ were prepared by conventional solid-state reaction by mixing stoichiometric amounts of Nd_2O_3 and MnO_2. The Nd_2O_3 is very sensitive to carbon dioxide and moisture, and was dried before use at 1000 °C overnight. The obtained powders were heated in air at 1200 °C overnight. In order to avoid the formation of unwanted Mn^{4+} (i.e. $NdMnO_{3+\delta}$), the heating process was done in a nitrogen atmosphere. The temperature-dependent PXD experiments were performed on a Bruker-D8 diffractometer, using Cu-K_{α_1} radiation for $20^\circ < 2\theta < 65^\circ$ and a step size of $2\theta = 0.04^\circ$ with 30 s per step. The temperature was controlled using an Anton-Paar TDK-1600 with kapton windows either in air or in a vacuum of 10^{-2} mbar.

3. Experimental results

The crystal structure of $RMnO_3$ perovskites distorts from the cubic parent structure due to the small radius of the R-ion. The RO_3 sublattice originates from a fcc packing of anions, common to many ionic solids (such as MgO), by replacing the face centred anions by R^{3+}. This results in an oxygen sublattice of corner-sharing octahedra. Because the ionic size of R^{3+} is smaller than that of O^{2-}, the cubic scaffold distorts. The resulting cooperative buckling and tilting of the corner-sharing octahedra yield for $RMnO_3$ at room temperature the orthorhombic Pbnm symmetry (figure 1). These distortions are known as the $GdFeO_3$ distortions [8, 9]. Besides the rotations, the oxygen octahedra can distort due to the degeneracy of the high-spin d^4 configuration of the Mn^{3+} ions, without reducing the Pbnm symmetry further. Thus, one distinguishes two substructures

with orthorhombic space group Pbnm, denoted as the O- and O′-structures. For the O-structure, the distortion consists of $GdFeO_3$ rotations of the octahedra, and thus $c/\sqrt{2} > a$ and $a < b$. The O′-orthorhombic structure is obtained if a cooperative JT distortion superimposes on the rotation of the MnO_6 octahedra. Here, the relation between the unit cell parameters is $c/\sqrt{2} < a < b$ [10, 11]. Thus, one can distinguish between these two structures by comparing the a and $c/\sqrt{2}$ orthorhombic unit cell parameters.

In this paper we will show that these two types of cooperative distortions are related. We can vary the rotation by the ionic size of the R^{3+}-ion. We will show that the ordering temperature of the orbital degree of freedom increases significantly with decreasing R^{3+} ionic size, even though the magnitude of the JT distortion is not influenced by the R^{3+} ionic size.

We study the high-temperature structure of $NdMnO_3$ by performing PXD experiments in air and in vacuum in the temperature interval 300–1473 K. The transition from the O′ to O structure is expected to be reflected in the temperature dependence of the lattice parameters.

The structural refinement at RT was performed in space group Pbnm. We used the structural parameters taken from [6] as a starting point. The oxygen displacements and the Debye–Waller factors have a large influence on the intensities of the weak peaks of the powder patterns. The measured intensity to background ratio of these peaks is low, leading to difficulties in separating the contribution of the oxygen displacements from the contribution of the Debye–Waller factors. Therefore we cannot accurately refine the oxygen positions for a quantitative determination of the bond lengths and angles and thus of the JT distortion parameter and rotation parameter.

All peaks could be indexed with Pbnm symmetry at all temperatures over the entire range $20^\circ < 2\theta < 65^\circ$. Regardless of the precise refinement of the oxygen fractional coordinates, the positions of the peaks enable a refinement of the lattice parameters with high accuracy. Thus we performed our refinements by fixing the oxygen positions at the RT values taken from [6] and by refining the following parameters: scale factor, background coefficients, zero-point error, unit cell parameters and Gaussian parameters. The peak profiles were very well reproduced by a Gaussian peak shape. For all the measured patterns, the refinements proceeded smoothly, and we noted no indication for considering a different symmetry.

From the evolution of the lattice parameters, the structural change from the orbitally ordered O′ structure (with $c/\sqrt{2} < a < b$) to the orbital disordered O structure (with $a < c/\sqrt{2} < b$) can be easily identified. The temperature dependence of the lattice parameters a, b and $c/\sqrt{2}$ and of the cube root of the molecular volume $\sqrt[3]{V}$ are depicted in figure 2, for the measurements performed in air. These data show the presence of the O′ phase (filled symbols) up to 973 K, the coexistence of the O′ and O phases for $T = 1073$ and 1173 K and the pure O phase (open symbols) at $T = 1273$ K. The structural transition can be directly identified in the powder diffractograms (see figure 3) by the dramatic change in the refined peak positions from 973 to 1273 K. The positions of (0 2 1) and (2 0 0) reflections are reversed with increasing temperature from 973 to 1273 K as a result of reversing the ratio between the lattice parameters, i.e. from $c/(\sqrt{2}a) < 1$ to $c/(\sqrt{2}a) > 1$. The patterns collected at intermediate temperatures, i.e. 1073 and 1173 K, show the presence of peaks belonging to both O′ and O structures, indicating the coexistence of both phases in this temperature interval. By increasing the temperature from 1073 to 1173 K, the peak intensities corresponding to the O structure increase at the expense of the decrease of the peak intensities originating from the O′ structure. The diffraction patterns at 1073 and 1173 K were refined by including both phases. (In figure 2 the lattice parameters of both phases are indicated at 1073 and 1173 K.) The refined ratio between the O′ and O phases at 1073 and 1173 K changes from 2 : 1 to 1 : 2, respectively, suggesting a two-phase region. The discontinuity

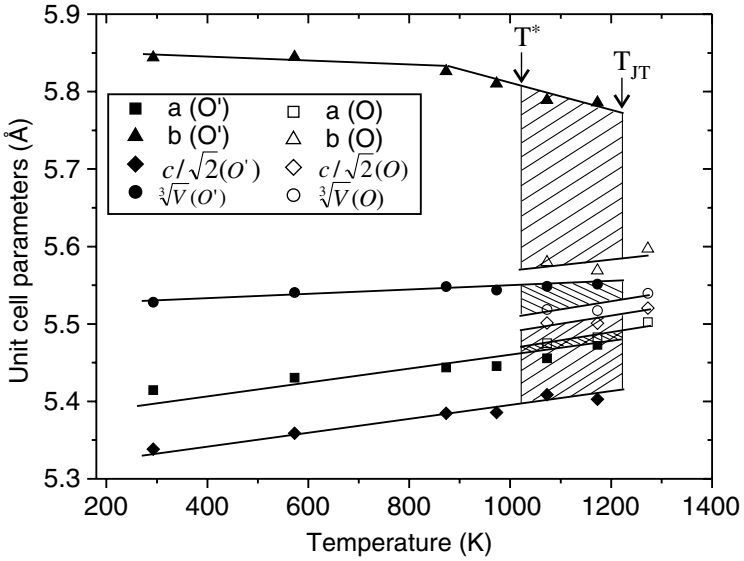

Figure 2. Temperature dependence of the unit cell parameters of $NdMnO_{3+\delta}$, measured in air. The lines are guides for the eye. The shaded area indicates the region in which the O′-orthorhombic phase (filled symbols) and O-orthorhombic phase (open symbols) coexist.

in the temperature dependence of the lattice parameters and of the molecular volume at the transition between the two phases indicates a first-order phase transition.

The structural phase transition is attributed to the orbital order–disorder transition, occurring in the temperature interval $\approx 1023 < T < 1223$ K. The coexistence of the O′ and O phases in a temperature interval is in agreement with an earlier structural study [4]. Furthermore, recent transport measurements [3] observed a large drop of the thermoelectric power over a temperature interval denoted by the authors as $T^* < T < T_{JT}$. The two temperatures, i.e. T^* and T_{JT}, are interpreted by them as the transition temperatures for the melting of the cooperative orbital ordering and for setting in of the short range orbital ordering of the occupied e_g orbitals of the MnO_6 octahedra, respectively. The differences in the transition temperature intervals reported in these studies, i.e. $873 < T < 1023$ K [4] and $800 < T < 1123$ K [3], compared with our results obtained from the measurements performed in air, i.e. $\approx 1023 < T < 1223$ K, can be the result of different amounts of Mn^{4+} impurities, due to differences in stoichiometry. Exposure to air at high temperatures will introduce non-JT active Mn^{4+} ions, which will reduce the orbital order–disorder transition temperatures. The coexistence of the O′- and O-orthorhombic phases over a temperature interval was also observed for $LaMnO_3$ [2], $PrMnO_3$ [5] and $SmMnO_3$ [4]. By comparing the results of the high-temperature structural study in $LaMnO_3$ with the results obtained in the detailed study of $La_{1-x}Ca_xMnO_3$, it can be inferred that the width of the temperature interval in which the two phases coexist, depends on x, decreasing from ≈ 200 K for $x = 0.19$ [12] to 10 K for $x = 0$ [2].

We analysed the effect of the Mn^{4+} ions on the JT transition by comparing the measurements performed in air with measurements performed in vacuum (10^{-2} mbar). We used the lattice parameters of the Pt-heater stripe sample holder and a Pt–Rh 10% thermocouple as temperature gauges. We observe that the temperature dependence of the lattice parameters of the platinum in both air and vacuum is the same within the standard deviation. This shows that no systematic

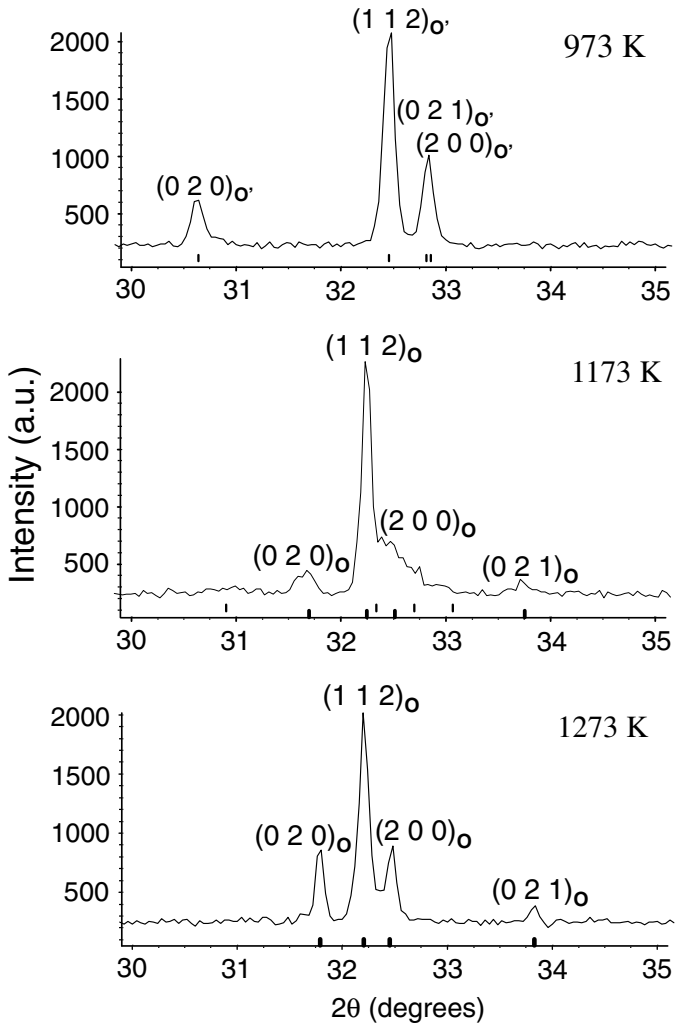

Figure 3. Selected range of the $NdMnO_3$ powder diffractograms collected in air at 973, 1173 and 1273 K. The full spectrum ranging from $20^\circ < 2\theta < 65^\circ$ was used for structural refinement. The refined peak positions are marked with thin and thick tick marks for the O′ and O structures, respectively. In the upper panel (973 K) the peaks are marked and labelled in the O′ structure. For diffractogram of the middle panel (1173 K), the O′ and O structures coexist in a ratio $\approx 1:2$ and the labels refer to the O phase. In the lower panel (1273 K) the peaks are marked and labelled in the O structure.

temperature errors occur between measurements in air and in vacuum. We notice that in vacuum, the orbital order–disorder transition in $NdMnO_3$ occurs in the temperature interval 1200–1400 K which is 200 K higher than the interval measured in air. This result is evidence that the measurements in air probe oxidized $NdMnO_{3+\delta}$ with $\delta \approx 0.2$. This introduces non-JT active Mn^{4+} ions. Although our results indicate that the measurements performed in vacuum are less sensitive to the formation of Mn^{4+}, in the following we will refer to the transition interval resulting from the measurements performed in air. This allows us to compare our results to the reports in the literature [1, 2, 4, 5].

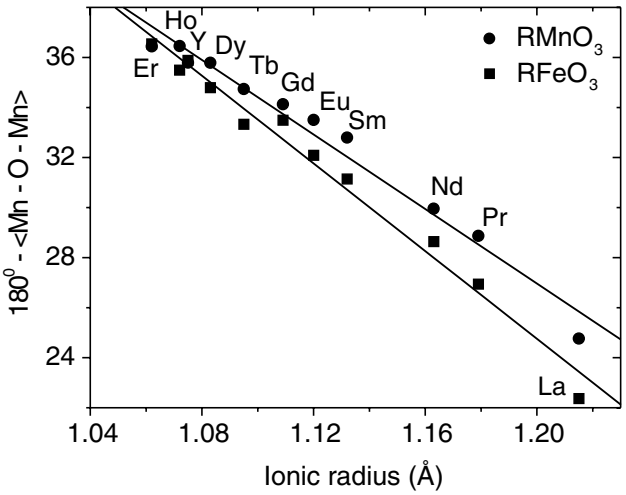

Figure 4. Rotation of the MnO_6 [6, 7] and FeO_6 [14] octahedra of $RMnO_3$ and $RFeO_3$, respectively, versus the R ionic radius at RT. The lines are guides for the eye.

As our data do not allow the refinement of the fractional coordinates of the oxygen positions, we cannot determine the temperature dependence of the rotation and JT distortion. However, from the evolution of the unit cell parameters we can conclude that the JT parameter decreases to zero at the temperature at which the orbital ordering is completely suppressed, i.e. 1273 K. This is analogous to $LaMnO_3$. The large difference between the a, b and $c/\sqrt{2}$ at 1273 K indicates a large rotation parameter above the transition. This is in contrast with the result obtained above T_{JT} in $LaMnO_3$ with $a \approx b \approx c/\sqrt{2}$ [1, 13]. This difference can be ascribed to the smaller ionic radius of Nd^{3+} than of La^{3+}.

4. Discussion

In order to understand the high temperature behaviour of the different $RMnO_3$ perovskites, we first discuss the evolution of the rotation and JT distortion of the oxygen octahedra with the size of the R ion. The RT structure of $RMnO_3$ (R = La, Pr, Nd, Sm, Eu, Gd, Tb, Dy, Ho, Y, Er) was studied in great detail by Alonso *et al* [6] and by Mori *et al* [7]. The contribution of each of the two parameters is obtained by comparing the $RMnO_3$ series with the non-JT series $RFeO_3$ [14].

The rotations of the octahedra are reflected in the deviation from 180° of the Mn–O–Mn tilting angle. The distortions associated with the JT effect are of two types and are denoted by Q2 and Q3. The Q3 is a tetragonal distortion which results in an elongation or a contraction of the MnO_6 octahedron corresponding to the filled $3z^2 - r^2$ orbital or $x^2 - y^2$ orbital, respectively. The Q2 is an orthorhombic distortion obtained by a certain superposition of the $3z^2 - r^2$ and $x^2 - y^2$ orbitals. The distortion modes characterizing the JT effect are defined as: $Q2 = 2(l - s)/\sqrt{2}$ and $Q3 = 2(2m - l - s)/\sqrt{6}$ with l and s the long and short Mn–O distances in the ab plane and m the medium out of plane Mn–O bond length [15, 16].

In figure 4 we plot the rotation parameter for $RMnO_3$ [6, 7] and $RFeO_3$ [14, 17] as a function of the size of the R-ion. The rotation parameter, defined as the deviation of the T–O–T tilting

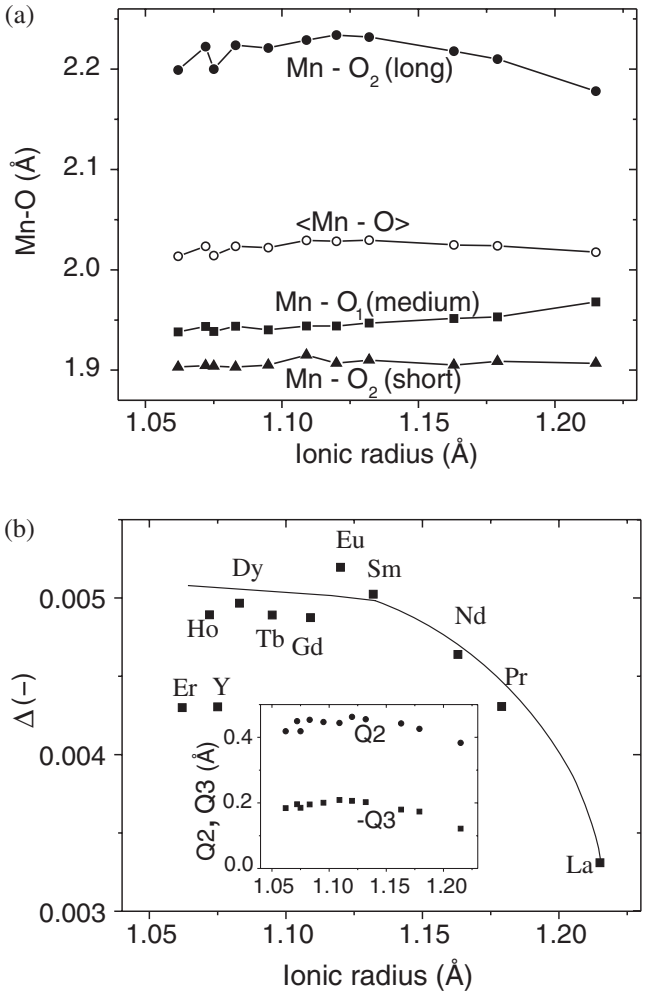

Figure 5. (a) Mn–O bond lengths and (b) JT distortion parameter Δ versus the R ionic radius of $RMnO_3$ at RT. The lines are guides for the eye. Inset: the Q2 and $-$Q3 components of the JT distortion versus the R ionic radius. We used the data from [6, 7].

angle from 180°, shows for both systems a linear increase with decreasing R-ionic radius. In figure 5(a) we plot the long (l), medium (m), short (s) and average Mn–O bond lengths versus the R-ionic radius. The medium bond length m deviates from the average bond length, such that $m < (l + s)/2$. This indicates that the JT distortion is not a purely Q2-type, but also partially Q3-type. Thus the distortion of the octahedra is defined by the deviation of the Mn–O distances from the average $\langle d \rangle$ value: $\Delta = (1/6) \sum_{n=1,6} [(d_n - \langle d \rangle)/\langle d \rangle]^2$ [16]. Figure 5(b) shows that Δ is similar for all R ions except for La^{3+}. The authors of [6] suggest that the deviation from the common value for $YMnO_3$ and $ErMnO_3$ results from the presence of significant amounts of Mn^{4+} ions due to the syntheses conditions (a O_2 flow was used to minimize the formation of the $RMnO_3$ hexagonal phase). The ionic size dependence of the Q2 and Q3 components of the JT distortion are shown in the inset of figure 5(b). We notice that for all the $RMnO_3$ perovskites, the Q2 component is dominant (with alternating long (l) and short (s) Mn–O_2 bond lengths in the

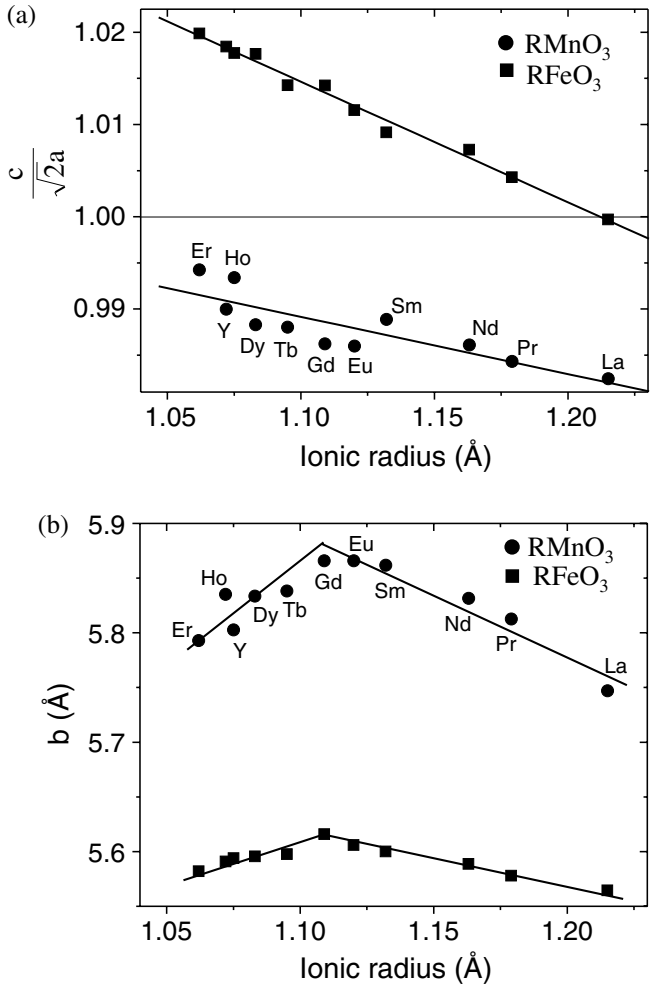

Figure 6. (a) Lattice parameter $c/(\sqrt{2}a)$ ratio and (b) b for $RMnO_3$ [6, 7] and $RFeO_3$ [14, 17] versus the R-ionic radius. The O′ structure shows $c/(\sqrt{2}a) < 1$ and O structure shows $c/(\sqrt{2}a) > 1$.

ab plane and a medium out-of-plane Mn–O_1 (m) bond length) and does not change significantly with the size of the R ion.

From the above relations we can evaluate the effect of the R-ionic radius on the lattice parameters in $RFeO_3$ [6, 7] and $RMnO_3$ [14, 17] shown in figures 6(a) and (b). In the $RFeO_3$ perovskites, the rotation distorts the parent cubic structure to the O structure with $b > c/\sqrt{2} > a$. Moreover, with decreasing R-ionic radius, the $c/(\sqrt{2}a)$ ratio increases, driven by the increased tilting of the octahedra. For the $RMnO_3$ perovskites, the cooperative JT distortion gives the O′ structure with $c/\sqrt{2} < a < b$. From figure 4, we observe that the rotation is similar for $RFeO_3$ and $RMnO_3$ for a given R. Thus the change in $c/(\sqrt{2}a)$ and b, is mainly affected by the JT distortion. The JT distortion for $RMnO_3$ perovskites is almost independent of the R-ionic size (see figure 5(b)). Figures 6(a) and (b) clearly show that the effect of the JT distortion is twofold: to increase the $c/(\sqrt{2}a)$ ratio by 0.02–0.03 and to increase significantly the b lattice parameter.

Finally, we discuss the effect of the R-ionic radius on the JT transition temperature (T_{JT}). Our high temperature measurements on $NdMnO_3$ are in agreement with previous measurements

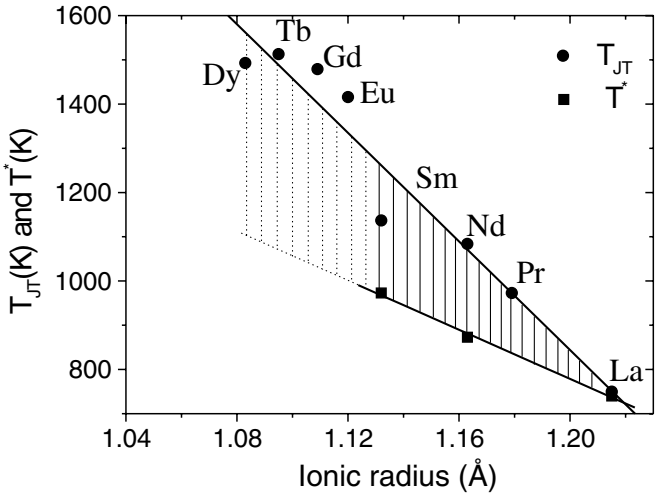

Figure 7. Orbital order–disorder transition temperatures T^* and T_{JT} versus the R-ionic radius in air. The hatched area represents the region where the orbitally ordered O′ phase coexists with the orbitally disordered O phase. The dotted hatched area represents an extrapolation to small R-ionic radii of this coexistence region. We used the data from [2] for $LaMnO_3$, from [5] for $PrMnO_3$ and from [4] for $NdMnO_3$ to $DyMnO_3$.

of different $RMnO_3$ [3]–[5]. This shows that the orbital order–disorder transition occurs over a temperature interval $T^* < T < T_{JT}$ in which the two Pbnm structures, i.e. O′ and O, coexist (the data were taken from [2, 4, 5]). We observe in figure 7 that the transition temperature T_{JT} increases with decreasing R-ionic size. However, the JT parameter Δ (figure 5(b)) shows a very small change with the R-ionic radius. The difference between the lattice parameters, i.e. a, b and $c/\sqrt{2}$ above T_{JT}, and thus the rotation above T_{JT}, increases with decreasing R-ionic radius. This shows that the rotation of the octahedra stabilizes the orbitally ordered state to higher temperatures. However, the magnitude of the JT distortion is not significantly affected by this rotation.

5. Conclusions

High-temperature x-ray powder diffraction of $NdMnO_3$ indicates that the orbital order–disorder transition takes place within a temperature interval of $1000 < T < 1200$ K. In this interval, the orbitally ordered O′ phase coexists with the orbitally disordered O phase. The discontinuity in the temperature dependence of the lattice parameters and of the molecular volume at the transition between the two phases proves a first-order phase transition. Moreover, we found that for the measurements performed in air, the orbital order–disorder transition occurs 200 K lower than for the measurements performed in vacuum. Thus the measurements in air probe an oxidized phase $NdMnO_{3+\delta}$, which introduces non-JT-active Mn^{4+} ions.

With decrease in R-ionic size, the orbital order–disorder transition temperatures T^* and T_{JT} increase significantly. In contrast, the magnitude of the JT distortion Δ shows a very small variation with the R-ionic radius. We conclude that the rotation of the MnO_6 octahedra is responsible for the stabilization of the cooperative JT distortion to higher temperatures.

Acknowledgment

This work is supported by the Netherlands Foundation for Fundamental Research on Matter (FOM).

References

[1] Rodriguez-Carvajal J, Hennion M, Moussa F, Moudden A H, Pinsard L and Revcolevschi A 1998 *Phys. Rev.* B **57** R3189
[2] Chatterji T, Fauth F, Ouladdiaf B, Mandal P and Ghosh B 2003 *Phys. Rev.* B **68** 052406
[3] Zhou J-S and Goodenough J B 2003 *Phys. Rev.* B **68** 144406
[4] Kasper N V and Troyanchuck I O 1996 *J. Phys. Chem. Solids* **57** 1601
[5] Pollert E, Krupička S and Kuzmičová E 1982 *J. Phys. Chem. Solids* **43** 1137
[6] Alonso J A, Martínez-Lopez M J, Casais M T and Fernández-Diaz M T 2000 *Inorg. Chem.* **39** 917
[7] Mori T, Kamegashira N, Aoki K, Shishido T and Fukuda T 2002 *Matter Lett.* **54** 238
[8] Hervieu M, Martin C, Maignan A, Van-Tendeloo G and Raveau B 1999 *Eur. Phys. J.* B **10** 397
[9] Maignan A, Martin C, Van-Tendeloo G, Hervieu M and Raveau B 1999 *Phys. Rev.* B **60** 15214
[10] Goodenough J B and Longo J M 1970 *Landolt-Börnstein Tabellen; New Series III/4a* (Berlin: Springer)
[11] Goodenough J B 1975 *Prog. Solid State Chem.* **5** 145
[12] van Aken B B, Meetsma A, Tomioka Y, Tokura T and Palstra T T M 2003 *Phys. Rev. Lett.* **90** 66403
[13] Norby P, Krogh Andersen I G and Krogh Andersen E 1995 *J. Solid State Chem.* **119** 191
[14] Marezio M, Remeika J and Dernier P 1970 *Acta Crystallogr.* B **26** 2008
[15] Kugel K I and Khomskii D I 1982 *Usp. Fiz. Nauk* **136** 621
[16] Kanamori J 1960 *J. Appl. Phys.* **31** 14S
[17] Boulay D, Maslen E N, Streltsov V A and Ishizawa N 1983 *Acta Crystallogr.* B **39** 921